doi:10.1093/brain/awz214 BRAIN 2019: 142; 3294–3305 | 3294

BRAIN
A JOURNAL OF NEUROLOGY

Dysregulated oscillatory connectivity in the visual system in autism spectrum disorder

Robert A. Seymour,[1,2,3] Gina Rippon,[1] Gerard Gooding-Williams,[1] Jan M. Schoffelen[4] and Klaus Kessler[1]

Autism spectrum disorder is increasingly associated with atypical perceptual and sensory symptoms. Here we explore the hypothesis that aberrant sensory processing in autism spectrum disorder could be linked to atypical intra- (local) and interregional (global) brain connectivity. To elucidate oscillatory dynamics and connectivity in the visual domain we used magnetoencephalography and a simple visual grating paradigm with a group of 18 adolescent autistic participants and 18 typically developing control subjects. Both groups showed similar increases in gamma (40–80 Hz) and decreases in alpha (8–13 Hz) frequency power in occipital cortex. However, systematic group differences emerged when analysing intra- and interregional connectivity in detail. First, directed connectivity was estimated using non-parametric Granger causality between visual areas V1 and V4. Feedforward V1-to-V4 connectivity, mediated by gamma oscillations, was equivalent between autism spectrum disorder and control groups, but importantly, feedback V4-to-V1 connectivity, mediated by alpha (8–13 Hz) oscillations, was significantly reduced in the autism spectrum disorder group. This reduction was positively correlated with autistic quotient scores, consistent with an atypical visual hierarchy in autism, characterized by reduced top-down modulation of visual input via alpha-band oscillations. Second, at the local level in V1, coupling of alpha-phase to gamma amplitude (alpha-gamma phase amplitude coupling) was reduced in the autism spectrum disorder group. This implies dysregulated local visual processing, with gamma oscillations decoupled from patterns of wider alpha-band phase synchrony (i.e. reduced phase amplitude coupling), possibly due to an excitation-inhibition imbalance. More generally, these results are in agreement with predictive coding accounts of neurotypical perception and indicate that visual processes in autism are less modulated by contextual feedback information.

1 Aston Brain Centre, School of Life and Health Sciences, Aston University, Birmingham, B4 7ET, UK
2 ARC Centre of Excellence in Cognition and Its Disorders, Macquarie University, Sydney, Australia
3 Department of Cognitive Science, Macquarie University, Sydney, Australia
4 Radboud University Nijmegen, Donders Institute for Brain, Cognition and Behaviour, Centre for Cognitive Neuroimaging, The Netherlands

Correspondence to: Klaus Kessler
School of Life and Health Sciences, Aston University, Aston Triangle, Birmingham, B4 7ET, UK
E-mail: k.kessler@aston.ac.uk

Correspondence may also be addressed to: Robert Seymour
E-mail: seymourr@aston.ac.uk

Keywords: ASD; visual system; oscillations; phase-amplitude coupling; Granger causality connectivity

Abbreviations: AQ = autism quotient; ASD = autism spectrum disorder; DAI = directed asymmetry index; GBA = gamma band activity; GSQ = Glasgow Sensory Questionnaire; MEG = magnetoencephalography; PAC = phase amplitude coupling

Received November 23, 2018. Revised May 2, 2019. Accepted May 20, 2019. Advance Access publication August 13, 2019

Introduction

Autism spectrum disorder (ASD) is a life-long neurodevelopmental condition, characterized by impairments in social interaction and communication, and the presence of repetitive patterns of behaviours, interests or activities (APA, 2013). Although these features remain the primary diagnostic markers of ASD, the presence of sensory symptoms have recently been given a more central role, consistent with findings of autism-related individual differences in visual perception (Robertson and Baron-Cohen, 2017). Additionally, >90% of ASD individuals experience hyper- and/or hypo-sensitive responses to certain stimuli, which can result in sensory overload (Leekam *et al.*, 2007). Differences in central coherence, local/global biases and predictive coding have all been proposed as possible mechanisms for these sensory symptoms (Happé, 2005; Mottron *et al.*, 2006; Pellicano and Burr, 2012). An understanding of the neural circuits involved will prove fruitful for ASD research, and could even provide early diagnostic markers (Roberts *et al.*, 2010; Kessler *et al.*, 2016).

Dysregulated neural oscillations—rhythmical changes in neural activity—are a promising neural correlate of atypical perceptual processes in autism (reviewed in Kessler *et al.*, 2016; Simon and Wallace, 2016). In particular, there has been increasing interest in characterizing patterns of atypical high-frequency gamma-band activity (GBA, >40 Hz) in ASD. Gamma oscillations play an important role in 'temporal binding' during sensory processing—the formation of a coherent percept essential for accurate information processing. GBA has therefore been proposed as a useful candidate frequency for studying temporal binding deficits in ASD alongside sensory symptoms more generally (Brock *et al.*, 2002). At the cellular level, gamma oscillations are generated through the co-ordinated interactions between excitatory and inhibitory populations of neurons (Buzsáki and Wang, 2012). Therefore, findings of abnormal GBA in ASD would link with theories of an excitation-inhibition imbalance and atypical connectivity in ASD (Rippon *et al.*, 2007).

As hypothesized, early studies of visual processing in ASD reported atypical, localized GBA responses to 'task relevant' stimuli as well as non-discriminant GBA increases to 'task irrelevant' stimuli (Grice *et al.*, 2001; Brown *et al.*, 2005). This was interpreted as an inability to synchronize visual responses at gamma frequencies, and bind perceptual processes into a coherent whole (Brock *et al.*, 2002). A later study by Sun *et al.* (2012), using magnetoencephalography (MEG), reported reduced gamma coherence in ASD participants viewing Mooney faces. Reduced gamma coherence in the visual cortex was also reported by Peiker *et al.* (2015*a*), who used a paradigm requiring the identification of moving objects presented through a narrow slit, necessitating the integration of perceptual information across time. However, another study by the same group, reported greater modulation of total gamma power in response to visual motion intensity for ASD participants (Peiker *et al.*, 2015*b*). Furthermore an MEG study using a higher-level visuospatial reasoning task in young children, reported increased patterns of gamma-band coherence between occipital and frontal sensors in ASD (Takesaki *et al.*, 2016). Whilst there is clear evidence of anomalous GBA during visual processing in ASD, the exact nature of these anomalies remains unclear: both increases and decreases in gamma-band power and coherence have been reported (reviewed in Kessler *et al.*, 2016; Simon and Wallace, 2016). We suggest that shifting the focus from within-band oscillatory power towards considering oscillation-mediated functional connectivity and between-band oscillatory relationships could help with understanding oscillopathies in ASD in more detail (Kessler *et al.*, 2016; Simon and Wallace, 2016).

Functional connectivity has been proposed as a unifying framework for autism, with the predominant theory emerging from functional MRI data being a global reduction but local increase in connectivity (Courchesne and Pierce, 2005; Hughes, 2007). Recent M/EEG research has supported the first of these claims with reductions in global connectivity during set-shifting, slit-viewing, face processing and whole-brain resting state studies (Doesburg *et al.*, 2013; Khan *et al.*, 2013; Kitzbichler *et al.*, 2015; Peiker *et al.*, 2015*a*, *b*). These reductions in connectivity are generally tied to feedback processes, located within the frontal lobes, and mediated by oscillations in theta (3–6 Hz), alpha (8–13 Hz) and beta bands (13–30 Hz). A recent study showed that during somatosensory stimulation, feedforward connectivity from primary to secondary somatosensory cortex is increased in ASD (Khan *et al.*, 2015). This suggests that feedforward pathways in the autistic brain may be over-compensating for the lack of feedback connectivity. At the local level, M/EEG studies (Khan *et al.*, 2013; reviewed in Kessler *et al.*, 2016) have not consistently supported the local increase in connectivity reported using functional MRI (Keown *et al.*, 2013). While some studies have identified patterns of GBA consistent with localized hyper-reactivity (Orekhova *et al.*, 2007; Cornew *et al.*, 2012), other studies report results consistent with reduced connectivity at the local as well as the global level (Khan *et al.*, 2013). One key issue to be considered is the validity of the spectral measures of connectivity being used, as inferences based on power measures alone can be inconsistent with more complex measures of coherence/phase-locking (Port *et al.*, 2015) or of cross-frequency coupling (Canolty and Knight, 2010).

An emerging biologically-relevant proxy for local connectivity is the coupling of oscillations from different frequency bands, termed cross-frequency coupling (Canolty and Knight, 2010; Seymour *et al.*, 2017). In particular, phase amplitude coupling (PAC) has been proposed to act as a mechanism for the dynamic co-ordination of brain activity over multiple spatial scales, with the amplitude of high frequency activity within local ensembles coupled to large-scale patterns of low frequency phase synchrony

(Bonnefond *et al.*, 2017). Alpha-gamma PAC is also closely tied to the balance between excitatory and inhibitory (E-I) populations of neurons (Mejias *et al.*, 2016), which is affected in autism (Rubenstein and Merzenich, 2003). One previous study has reported dysregulated alpha-gamma PAC in the fusiform face area during emotional face processing in autistic adolescents (Khan *et al.*, 2013). Local PAC was also related to patterns of global alpha hypoconnectivity in autism, suggesting that local and global connectivity are concurrently affected. Altogether, oscillation-based functional connectivity in autism is characterized by local dysregulation and global hypoconnectivity (Kessler *et al.*, 2016).

Within the context of visual processing, this view leads to several hypotheses, outlined in Kessler *et al.* (2016). Electrocorticography (ECoG) recordings in macaques and MEG in humans suggest that visual oscillations in different frequency bands have distinct cortical communication profiles. Gamma-band oscillations pass information up the visual hierarchy, in a feedforward manner, whereas alpha and beta-band oscillations mediate feedback connectivity down the cortical hierarchy (Bastos *et al.*, 2015*a, b*; Michalareas *et al.*, 2016). Long-range alpha/beta connectivity has also been linked with top-down attentional processes during visual perception via the regulation of local gamma oscillations (Klimesch, 2012; Richter *et al.*, 2017) and of local alpha-gamma PAC (Chacko *et al.*, 2018). Hypothesizing that autism is associated with alterations in directed functional connectivity (Khan *et al.*, 2015), we predict reduced feedback connectivity within the visual system, mediated by oscillations in the alpha band, but potentially increased feedforward connectivity in the gamma band (Kessler *et al.*, 2016). At the local level, neurotypical visual processing is accompanied by increases in alpha-gamma PAC, thought to arise through the E-I coupling between infragranular and supragranular layers of visual cortex (Mejias *et al.*, 2016; Bonaiuto *et al.*, 2018). Given an E-I imbalance in autism and reported local dysregulation of cortical activity, we hypothesize reduced alpha-gamma PAC within primary visual cortex in ASD participants (Khan *et al.*, 2013; Kessler *et al.*, 2016). Finally, if top-down alpha connectivity has a modulatory effect on bottom-up processing, then local alpha oscillations and alpha-gamma PAC, e.g. in V1, could reveal a systematic relationship with top-down alpha connectivity, e.g. from V4 (Khan *et al.*, 2013). This may present itself differently between groups, with a more variable relationship between feedback connectivity and local PAC in the ASD group (Dinstein *et al.*, 2012).

We tested these hypotheses using MEG, which combines excellent temporal resolution with sophisticated source localization techniques (Van Veen *et al.*, 1997; Hillebrand and Barnes, 2005). A group of 18 adolescent ASD participants and 18 typically developing control subjects performed an engaging visual task, to induce alpha and gamma oscillations. We characterized changes in power and connectivity between visual areas V1 and V4: two regions with strong hierarchical connectivity (Bastos *et al.*, 2015*a*, *b*; Michalareas *et al.*, 2016). Additionally, we quantified local alpha-gamma PAC for V1 (Cohen, 2008; Özkurt and Schnitzler, 2011; Seymour *et al.*, 2017).

Methods and materials

Participants

Data were collected from 18 participants diagnosed with ASD and 18 age-matched typically developing control subjects (Table 1). ASD participants had a confirmed clinical diagnosis of ASD or Asperger's syndrome from a paediatric psychiatrist. Participants were excluded if they were taking psychiatric medication or reported epileptic symptoms. Control participants were excluded if a sibling or parent was diagnosed with ASD. Data from a further nine participants were excluded (Supplementary material).

Experimental procedures

Experimental procedures complied with the Declaration of Helsinki and were approved by Aston University ethics committee. Participants and a parent/guardian gave written informed consent.

Behavioural assessments

General non-verbal intelligence was assessed using the Raven's Matrices Task (Raven and Court, 1998). The severity of autistic traits was assessed using the autism quotient (AQ; Baron-Cohen *et al.*, 2001*a*) and sensory traits using the Glasgow Sensory Questionnaire (GSQ; Robertson and Simmons, 2013). All 18 ASD participants, and 15 of 18 control participants completed

Table 1 Participant demographic and behavioural data

	n	Age	Male/ female	AQ (adult)/50	Raven Matrices Score/60	GSQ Score/168	Mind in the Eyes Score/36
ASD	18	16.67 (3.2) [14–20]	14/4	32.60* (6.64) [21–46]	43.84 (7.93) [27–56]	65.33* (27.69) [27–126]	21.88 (4.87) [12–30]
Control	18	16.89 (2.8) [14–20]	15/3	10.91 (5.43) [6–21]	48.71 (5.78) [37–56]	38.70 (6.88) [29–50]	25.44 (4.03) [17–33]

Values are presented as *n* or mean (SD) [range].
*Behavioural scores significantly greater in ASD > control group, *t*-test, $P < 0.05$.

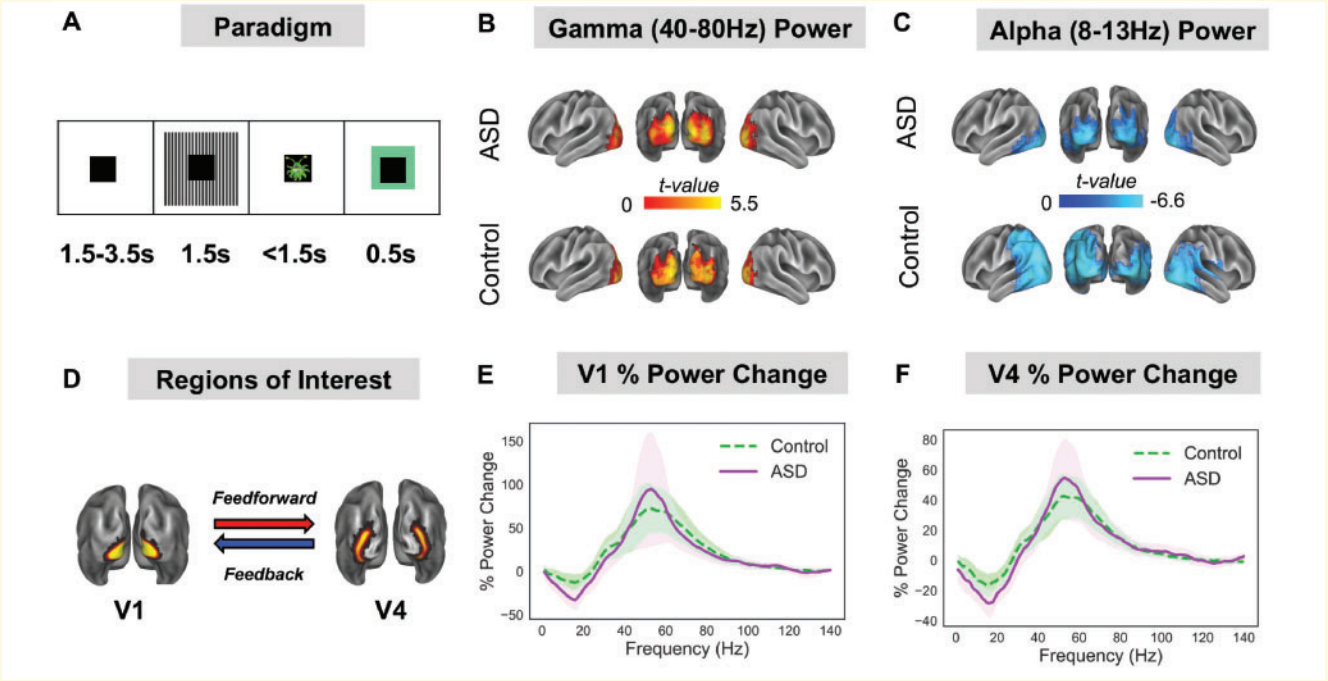

Figure 1 Experimental Protocol and region of interest power analysis. (**A**) Participants performed a visual task, consisting of 1.5–3.5 s baseline period followed by 1.5 s presentation of a visual grating. After the grating, participants were presented with a cartoon alien or astronaut picture and instructed to only respond when an alien was presented (response time up to 1.5 s). The alien/astronaut stimuli were to maintain attention and do not form part of the analysis. (**B** and **C**) The change in oscillatory power between grating and baseline periods was localized on a cortical mesh and masked to show only statistically significant ($P < 0.05$, corrected) stimulus induced increases in gamma (40–80 Hz) and decreases in alpha (8–13 Hz) power. There were no statistically significant differences in relative gamma or alpha power between groups (see Supplementary Fig. 1 for a whole-brain comparison). (**D**) Regions of interest in V1 and V4 were defined using HCP-MMP 1.0 atlas. (**E** and **F**) The change in power between grating and baseline periods was calculated for V1 and V4 from 1–140 Hz. Results show characteristic reductions in alpha/beta power and increases in gamma-band power (40–80 Hz) for V1 and V4. There were no statistically significant differences in power between groups. The shaded area around each curve indicates 95% confidence intervals.

the questionnaires. AQ and GSQ scores were significantly higher in the ASD group (Table 1). Participants also completed the Mind in the Eyes test (Baron-Cohen *et al.*, 2001*b*); however, there were no group differences. The Mind in the Eyes test has been criticized for measuring emotion recognition rather than an autism-specific deficit in mental state attribution (Oakley *et al.*, 2016), and therefore these scores were not analysed further.

Paradigm

Whilst undergoing MEG, participants performed a sensory task (Fig. 1A), designed to elicit gamma-band oscillations. Each trial started with a randomized fixation period (1.5, 2.5 or 3.5 s), followed by the presentation of a visual grating or auditory binaural click train stimulus; however only visual data will be analysed in this article. The visual grating had a spatial frequency of 2 cycles/degree and was presented for 1.5 s. To promote task engagement, cartoon pictures of aliens or astronauts were presented after the visual grating for 0.5 s, but did not form part of the MEG analysis. Participants were instructed to respond to the appearance of an alien picture using a response pad (maximum response period of 1.5 s). The accuracy of the response was conveyed through audiovisual feedback, followed by a 0.5 s fixation period. MEG recordings lasted 12–13 min and included 64 trials with visual grating stimuli. Accuracy rates were >95% for all participants.

MEG and MRI acquisition

MEG data were acquired using a 306-channel Neuromag MEG device (Vectorview, Elekta). A structural T_1 brain scan was acquired for source reconstruction using a Siemens MAGNETOM Trio 3 T scanner. MEG sensors were co-registered with anatomical MRI data by matching the digitized head-shape data with surface data from the structural scan (Jenkinson and Smith, 2001). For each participant, a cortical mesh was constructed using Freesurfer v5.3 (Fischl, 2012), and registered to a standard fs_LR mesh (Van Essen, 2012). For more detailed instructions, see the online Supplementary material.

MEG preprocessing

MEG data were preprocessed using Maxfilter [temporo-spatial signal separation (tSSS), 0.9 correlation], which supresses external sources of noise (Taulu and Simola,

2006). Further preprocessing was performed in MATLAB 2014b using the Fieldtrip toolbox v20161024 (Oostenveld *et al.*, 2010). Data were band-pass filtered (0.5–250 Hz, Butterworth filter) and band-stop filtered (49.5–50.5 Hz; 99.5–100.5 Hz) to remove power-line contamination and harmonics. Data were epoched into segments of 4 s (1.5 s pre-, 1.5 s post-stimulus onset, with ±0.5 s padding), demeaned and detrended. Trials containing artefacts (SQUID jumps, eye-blinks, head movement, muscle) were removed if the trial-by-channel magnetomer variance exceeded 8×10^{-23}. This resulted in a group average of 60.2 trials for the ASD group and 61.9 trials for the control group. Four noisy MEG channels were removed from all analyses.

Source-level power

Source analysis was carried out using a linearly constrained minimum variance beamformer (Van Veen *et al.*, 1997), which applies a spatial filter to the MEG data at each vertex of the cortical mesh. Because of differences in noise between sensor types, covariance matrix terms resulting from multiplying magnetomer and gradiometer data were removed. Beamformer weights were calculated by combining this covariance matrix with leadfield information, with data pooled across baseline and grating periods. Following tSSS, sensor-level data had a rank 64 or below, and therefore a regularization parameter of lambda 5% was applied. Data were band-pass filtered between 40–80 Hz (gamma) and 8–13 Hz (alpha), and source analysis was performed separately. While gamma is typically defined as a wider range of frequencies, here we focused on a 40–80 Hz subrange for an optimal signal-to-noise ratio for source localization. To capture induced rather than evoked visual power, a period of 0.3–1.5 s following stimulus onset was compared with a 1.2 s baseline period (1.5–0.3 s before grating onset).

Region of interest definition

To quantify directed connectivity within the visual system, we selected two regions of interest: visual area 1 (V1) and visual area 4 (V4), defined using HCP-MMP 1.0 atlas (Glasser *et al.*, 2016) (Fig. 1C). Both regions show stimulus-related changes in oscillatory power (Fig. 1E and F) and demonstrate reliable patterns of hierarchical connectivity: V1-to-V4 connectivity is feedforward; whereas V4-to-V1 connectivity is feedback (Bastos *et al.*, 2015*a*, *b*; Michalareas *et al.*, 2016). Twelve vertices from posterior V1 were excluded to ensure clear anatomical separation of the regions of interest. To obtain a single spatial filter for each region of interest, we performed a principal components analysis on the concatenated filters encompassing V1 and V4, multiplied by the sensor-level covariance matrix, and extracted the first component (Schoffelen *et al.*, 2017). Broadband (0.5–250 Hz) sensor-level data were multiplied by this spatial filter to obtain 'virtual electrodes'. Finally, the change in oscillatory power between grating and baseline periods was calculated using multi-tapers (Hoogenboom *et al.*, 2006) from 1–140 Hz, 0.5 s time window, sliding in steps of 0.02 s and ±8 Hz frequency smoothing.

V1-V4 directed connectivity

To quantify V1-V4 directed functional connectivity, we used a spectrally resolved non-parametric version of Granger causality—a statistical technique that measures the extent to which one time series can predict another (Granger, 1969; Dhamala *et al.*, 2008). Data from V1 and V4 (0.3–0.15 s post-stimulus onset) were split into 0.4-s epochs to enhance the accuracy of results, Fourier transformed (Hanning taper; 2 Hz smoothing), and entered into a non-parametric spectral matrix factorization procedure. Granger causality was then estimated between 1–140 Hz for each region of interest pair and averaged across hemispheres. To create surrogate data (with no interregional connectivity), 0.4-s long time series were produced with the same spectral properties as V1/V4, modelled using the first autoregressive coefficient (Colclough *et al.*, 2015; see Supplementary material for MATLAB code). Granger causality was estimated between these surrogate V1-V4 time series using the same procedure as for the actual data. Granger causality spectra from the actual data were compared with surrogate Granger causality spectra using cluster-based permutation tests (see 'Statistical analysis' section).

Asymmetries in Granger causality values were quantified using a directed asymmetry index (DAI), originally defined in Bastos *et al.* (2015*b*):

$$DAI = \frac{GC(V1 \rightarrow V4) - GC(V4 \rightarrow V1)}{GC(V1 \rightarrow V4) + GC(V4 \rightarrow V1)} \quad (1)$$

This results in normalized values (−1 to +1) for every frequency bin, with values >0 indicating feedforward Granger causality influence and values <0 indicating feedback influence. DAI values were statistically compared between groups.

Phase amplitude coupling

V1 time courses were examined for changes in alpha-gamma PAC. For detailed discussion about PAC computation and methodological issues see Seymour *et al.* (2017). Briefly, we calculated PAC between 7–13 Hz phase (1 Hz steps) and amplitudes 34–100 Hz (in 2 Hz steps), from 0.3–1.5 s post-grating presentation. PAC values were corrected using 1.2 s of data from the baseline period. In accordance with Seymour *et al.* (2017), we used a wide amplitude frequency range (34–100 Hz) to characterize which gamma frequencies give rise to maximum changes in PAC (i.e. a data-driven approach). Thirty-four hertz was chosen as the lower limit of the range, as this is the lowest detectable amplitude frequency for phases from 7 to 13 Hz. Amplitude-phase co-modulograms (size: 33 × 7), were

statistically compared between groups using cluster-based permutation testing (Maris and Oostenveld, 2007).

PAC was calculated using two separate approaches, a mean vector length algorithm (Özkurt and Schnitzler, 2011), MVL-Ozkurt, and a phase-locking algorithm (Cohen, 2008), PLV-Cohen. This decision was based on our previous study that compared the efficacy of four different PAC algorithms for MEG data analysis (Seymour *et al.*, 2017). Additional details are outlined in the Supplementary material, and code used for PAC computation is available at: https://github.com/neurofractal/sensory_PAC.

Statistical analysis

Statistical analysis was performed using cluster-based permutation tests (Maris and Oostenveld, 2007), which consist of two parts: first an independent-samples *t*-test is performed, and values exceeding an uncorrected 5% significance threshold are grouped into clusters. The maximum *t*-value within each cluster is carried forward. Second, a null distribution is obtained by randomizing the condition label (e.g. ASD/control) 1000 times and calculating the largest cluster-level *t*-value for each permutation. The maximum *t*-value within each original cluster is then compared against this null distribution, and the null hypothesis is rejected if the test statistic exceeds a threshold of $P < 0.05$. Cluster-based permutation tests are an effective way to address the multiple-comparison problem for neuroimaging data, which is especially problematic for M/EEG data analysed over frequency, time and space (Maris and Oostenveld, 2007).

Data availability

The data that support the findings of this study are available on reasonable request from corresponding author, R.S., in a preprocessed and de-anonymized form. The raw data are not publicly available due to ethical restrictions. MATLAB data analysis code for this study will be made available openly on Github. Code for PAC computation is openly available at: https://github.com/neurofractal/sensory_PAC.

Results

Oscillatory power

The change in oscillatory power following presentation of the visual grating, versus baseline, was calculated on a cortical mesh for the alpha (8–13 Hz) and gamma (40–80 Hz) bands. For both ASD and control groups there was a statistically significant relative increase in gamma power (Fig. 1B) and a relative decrease in alpha power (Fig. 1C), localized to the ventral occipital cortex. This replicates previous MEG/EEG studies using visual grating stimuli (Hoogenboom *et al.*, 2006; Michalareas *et al.*, 2016). Interestingly, there were no significant differences in relative gamma or alpha power between groups ($P > 0.05$, Supplementary Fig. 1).

Two regions of interest were defined in V1 and V4 (Fig. 1D). Changes in oscillatory power (grating versus baseline) from V1 (Fig. 1E) and V4 (Fig. 1F) showed characteristic increases in gamma-band power (40–80 Hz) and decreases in alpha/beta power (8–20 Hz). Between groups, there were minor differences between the power spectra, including a larger alpha/beta induced power change for the ASD group (Fig. 1E and F, purple line) but none of these differences were significant (both $P > 0.05$).

In sum, we found no evidence for group differences (control versus ASD) in gamma or alpha relative oscillatory power following the presentation of a visual grating. Additionally, there were no significant correlations between oscillatory power in V1/V4 and behavioural AQ scores for the ASD group (Supplementary Fig. 2).

Feedforward/feedback connectivity

The directed functional connectivity between V1 and V4 was quantified using Granger causality. Across groups, all reported increases in bidirectional V1-V4 Granger causality were greater than for surrogate data (Supplementary Fig. 3). For the control group (Fig. 2A), V1-to-V4 (henceforth termed feedforward) connectivity showed a prominent increase from 40–80 Hz in the gamma band. In contrast, V4-to-V1 (henceforth termed feedback) connectivity showed a prominent increase from 8–13 Hz in the alpha band (Fig. 2A). This dissociation between feedforward gamma and feedback alpha replicates previous findings in macaques and humans (Bastos *et al.*, 2015*b*; Michalareas *et al.*, 2016). The feedforward gamma-band peak (40–80 Hz) was also evident in the ASD Granger spectra (Fig. 2B, red line). There was a reduction in the alpha-band feedback peak in the ASD group compared with control subjects (Fig. 2B, blue line).

To quantify asymmetries in feedforward/feedback connectivity between groups, we calculated the DAI (see 'Materials and methods' section). The control group displayed a feedback peak from 0–20 Hz (negative DAI values) and feedforward peak from 40–80 Hz (positive DAI values). By statistically comparing DAI between groups, it was found that values from 8–14 Hz were significantly lower ($P = 0.032$) for the control group than the ASD group. All other frequencies, including gamma (40–80 Hz) showed similar DAI values between groups. This suggests reduced V4-to-V1 feedback connectivity for the ASD group, mediated by alpha-band oscillations (8–14 Hz), but typical V1-to-V4 feedforward connectivity mediated by gamma oscillations (40–80 Hz).

There was no feedforward Granger causality peak in the theta-band (4–8 Hz) for either the control or ASD group, as previously reported using ECoG (Spyropoulos *et al.*, 2018). This could be due to lower sensitivity of MEG recordings

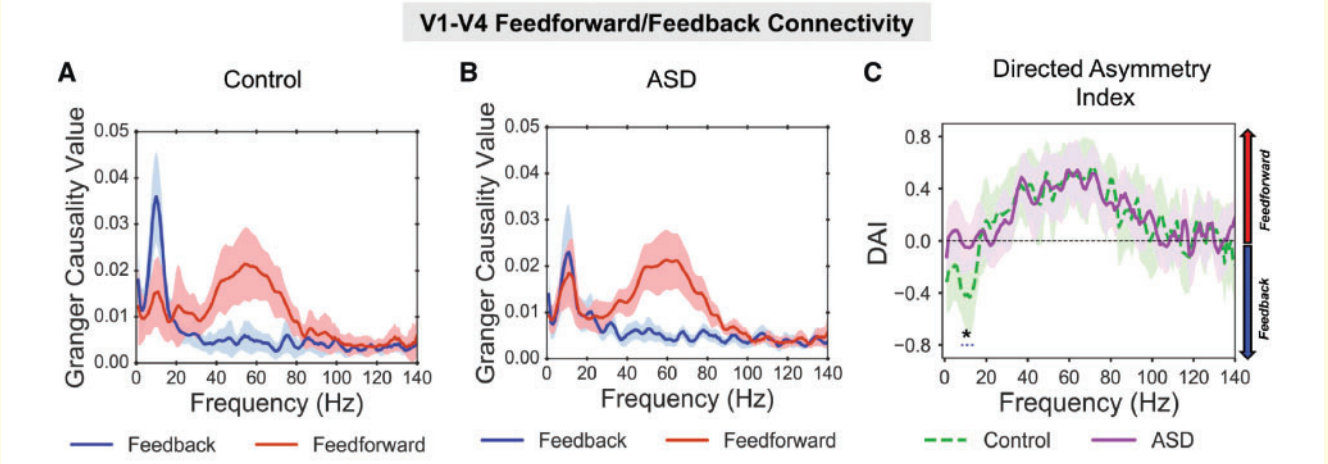

Figure 2 V1-V4 feedforward/feedback connectivity. (**A**) For the control group there was a peak in Granger causality values, in the gamma-band (40–80 Hz, red line) for V1-to-V4 feedforward connectivity, and a peak in Granger causality values in the alpha band (8–13 Hz, blue line) for V4-to-V1 feedback connectivity. (**B**) For the ASD group there was also a peak in Granger causality values in the gamma-band for V1-to-V4 feedforward connectivity; however, there was a smaller peak in Granger causality in the alpha-band for V4-to-V1 feedback connectivity. For comparisons with surrogate data per group, see Supplementary Fig. 3. (**C**) The difference between feedforward and feedback connectivity was quantified as the DAI. The difference in DAI between control (dashed, green line) and ASD (solid, purple line) was significant ($P = 0.036$), with lower DAI values ($P = 0.036$) between 8–14 Hz for the control group, suggesting reduced V4-to-V1 feedback connectivity in autism. The shaded area around each Granger causality line indicates 95% confidence intervals.

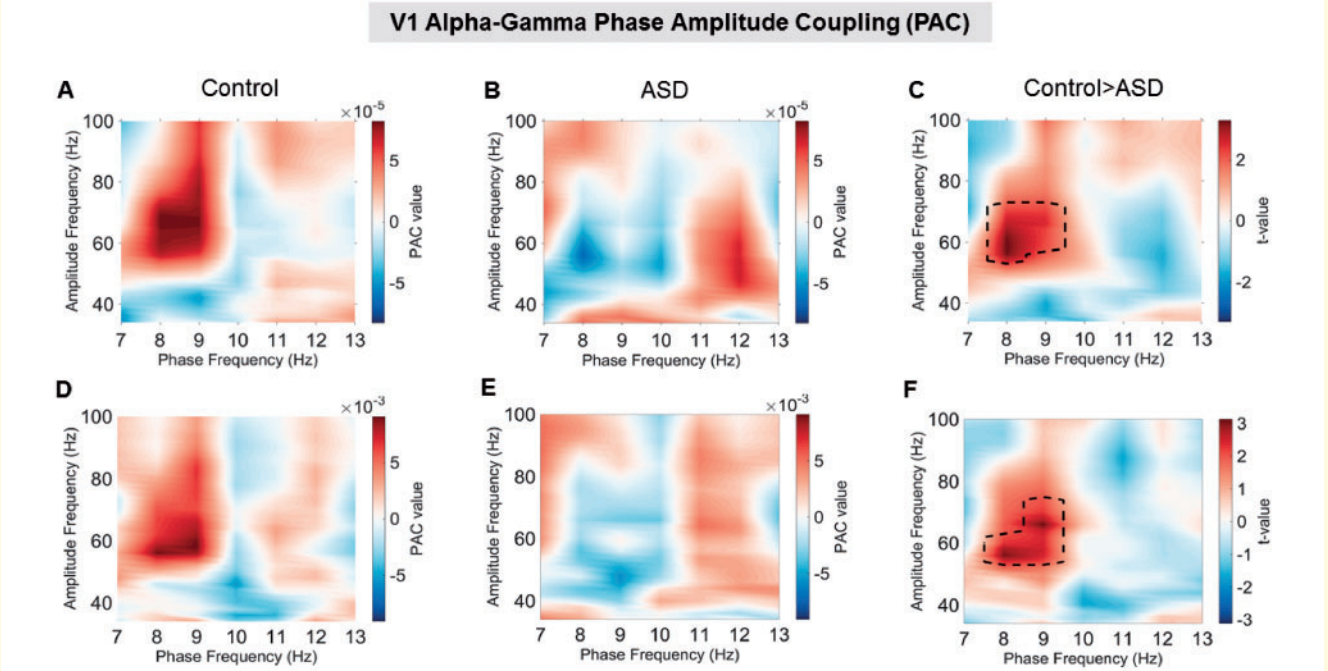

Figure 3 V1 phase amplitude coupling using the MVL-Özkurt (A–C) and the PLV-Cohen (D–F) approaches. (**A** and **D**) The control group showed increased alpha-gamma PAC compared with baseline, with a peak between 50–80 Hz amplitude and 7–9 Hz phase. (**B** and **E**) The ASD group showed less prominent increases in PAC with a much smaller peak from 40–70 Hz amplitude and 11–13 Hz phase shown in **B** and an even smaller peak shown in **E**. (**C** and **F**) Robust statistical comparison (see 'Materials and methods' section for details) indicated significantly larger PAC for the control compared to the ASD group ($P = 0.029$ in **C** and $P = 0.037$ in **F**) from 54–72 Hz amplitude and 8–9 Hz phase.

(Michalareas *et al.*, 2016), as well as the centrally-masked visual grating (Fig. 1A).

Alpha-gamma phase amplitude in V1

Activity from visual area V1 was examined for changes in alpha-gamma PAC using two separate approaches (MVL-Ozkurt and PLV-Cohen). Frequency co-modulograms showed increased PAC in the control group, peaking at 8–10 Hz phase frequencies and 50–70 Hz amplitude frequencies (Fig. 3A and D). These results replicate Seymour *et al.* (2017), who showed increased alpha-gamma PAC in an adult population using the same visual grating stimulus. The co-modulograms for the ASD group displayed lower PAC values, with no clear positive peak (Fig. 3B and E). Comparing control versus ASD groups, there was a single positive cluster of greater PAC between 8–9 Hz and 52–74 Hz for the MVL-Özkurt approach (Fig. 3C, $P = 0.029$); and a single positive cluster between 8–9 Hz and 54–74 Hz for the PLV-Cohen approach (Fig. 3F, $P = 0.037$). This suggests that the coupling between alpha and gamma oscillations during perception in primary visual cortex is reduced in autism. The similarity in PAC co-modulograms between MVL-Özkurt and PLV-Cohen approaches indicates that the results generalize across both PAC metrics.

Connectivity-behaviour correlation

Behavioural ASD data from the AQ and GSQ (Baron-Cohen *et al.*, 2001*a*; Robertson and Simmons, 2013) were correlated with group differences in alpha-band DAI and alpha-gamma PAC (Fig. 5). The AQ questionnaire measures general autistic traits, whilst the GSQ measures the level of reported sensory hypo- and hyper-sensitives across domains (Baron-Cohen *et al.*, 2001*a*; Robertson and Simmons, 2013). There was a significant positive correlation between AQ score and alpha DAI (Fig. 4B, $r = 0.526$, $P = 0.025$) suggesting that increased V4-to-V1 feedback connectivity (negative DAI values) is related to lower levels of autistic traits (lower AQ scores). There were no other significant correlations for the GSQ or PAC.

This analysis was repeated for the behavioural data from the control group. However, there were no significant correlations for any combination of DAI/PAC and AQ/GSQ data (Supplementary Fig. 5), $P > 0.05$.

Discussion

This study examined the oscillation-based functional connectivity within the visual system of autistic adolescents and typically developing age-matched control subjects. Confirming our hypotheses (Kessler *et al.*, 2016), we found a reduction in alpha-band (8–13 Hz) feedback connectivity from V4-to-V1 in the ASD group alongside a reduction in the coupling between alpha and gamma oscillations in V1, measured via PAC, suggesting dysregulation of local connectivity in autism. Further, in agreement with predictions (Kessler *et al.*, 2016), aberrant connectivity patterns were observed in the absence of significant group differences in oscillatory power changes relative to baseline (Fig. 1 and Supplementary Fig. 1).

Feedback/feedforward connectivity

By examining frequency-specific asymmetries in V1-V4 connectivity during visual processing (Bastos *et al.*, 2015*a b*; Michalareas *et al.*, 2016), this study found that the ASD group had specific reductions in feedback, but not feedforward, connectivity. This is consistent with previous MEG and functional MRI studies showing a reduction in global connectivity in autism (Hughes, 2007; Khan *et al.*, 2013; Kitzbichler *et al.*, 2015). Having said this, it should be acknowledged that connectivity between visual regions V1-V4 might be better characterized as 'interregional' rather than truly global. Future ASD-MEG research could examine global feedback/feedforward connectivity using measures of directed functional connectivity (e.g. Granger causality) in concert with higher level cognitive tasks involving a more extended set of cortical regions.

Using a simple visual paradigm, this study did not reveal an increase in connectivity from V1-to-V4 for the ASD group mediated by gamma oscillations, suggesting equivalent levels of feedforward information flow in the visual system between groups. Whilst Khan *et al.* (2015) reported increased feedforward connectivity in autism, they focused on somatosensory rather than visual processing with a younger group of adolescent participants. In any case, we hypothesize that where visual processing can be achieved via feedforward processes (reflected at gamma frequencies), autistic participants may perform on par or even outperform their typically developing peers (Mottron *et al.*, 2006). For example, during visual search tasks, autistic participants have been reported to perform faster than control subjects (Jobs *et al.*, 2018).

In contrast, we observed a reduction in feedback connectivity from V4 to V1 that was specific to alpha-band oscillations (8–14 Hz; Fig. 2). While a comparison with surrogate data (Supplementary Fig. 3) revealed a significant alpha feedback peak for the ASD group, it did not differ from the alpha feedforward peak, resulting in a DAI significantly closer to 0 than in the control group (Fig. 2C). Our data suggest that whilst relative alpha power was unaffected (Fig. 1C, E and F and Supplementary Fig. 1), the feedback flow of information from higher to lower visual regions was reduced in our ASD sample. A reduced ability to implement top-down modulation of bottom-up visual information may result in the atypical visual processes reported by many autistic individuals.

Despite observing no significant correlation between oscillatory power and AQ or GSQ at any frequency (Supplementary Fig. 2), a significant correlation was revealed between the reduction in alpha feedback connectivity and

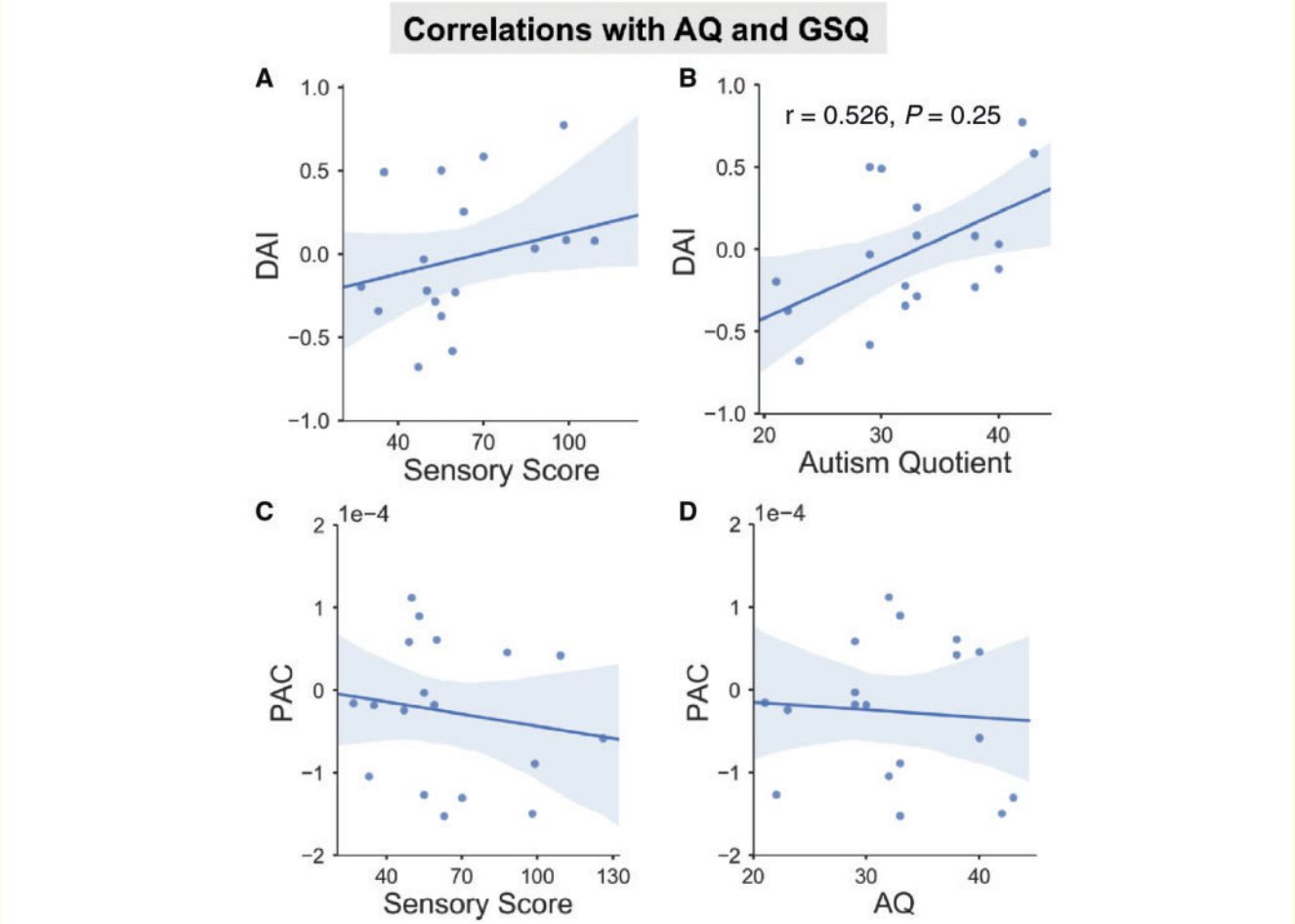

Figure 4 Correlations between questionnaire scores and brain measures. For the ASD group, the correlation between alpha-band DAI (**A** and **B**), alpha-gamma PAC (**C** and **D**) and AQ (**B** and **D**), GSQ (**A** and **C**) was plotted with regression line (95% confidence interval indicated by shaded region). (**B**) There was a positive correlation between DAI and AQ score.

AQ score in the ASD group, further supporting our hypothesis of decreased top-down connectivity in ASD. However, we did not find a corresponding correlation with GSQ score that would corroborate our hypothesis with respect to the severity of sensory symptoms. A possible reason for the lack of correlation could be that the GSQ is a general questionnaire, which addresses aberrations across seven sensory domains (visual, auditory, gustatory, olfactory, tactile, vestibular, proprioceptive) at the expense of an in-depth assessment of any specific modality. In addition, different items per domain address either hypo- or hyper-sensitivities (resulting in only three items per expression, per domain) and the obtained scores in our sample indeed reflect a mix between both symptom expressions (Supplementary Fig. 6). This and the observation that sensory symptoms were only reported as 'rarely' or 'sometimes' in our sample, may have added to a variable relationship between brain measures and GSQ scores. In conclusion, brain-behaviour relationships might be better assessed using more precise psychophysical tests of visual perception (Ashwin *et al.*, 2009), combined with formal clinical assessments.

Phase amplitude coupling

Within primary visual cortex (V1), there was a reduction in alpha-gamma PAC for the ASD group (Fig. 3). It is important to note that the group differences in PAC arose despite similar relative changes in gamma and alpha power (Fig. 1). Interestingly, one previous ASD study reported reduced inter-regional connectivity and local alpha-gamma PAC during face processing, despite similar event-related activity and oscillatory power between groups (Khan *et al.*, 2013). As reviewed in the 'Introduction', reports of gamma band responses (GBA) in ASD are inconsistent, with some M/EEG studies reporting hyper-reactivity (Orekhova *et al*, 2007; Cornew *et al*, 2012), while others report reduced GBA at the local level (Khan *et al*, 2013). Future studies should therefore explore the precise regulation of gamma oscillations via cross-frequency coupling, rather than relying on measures of power alone (Canolty and Knight, 2010; Kessler *et al.*, 2016; Simon and Wallace, 2016).

PAC has been reported to rely heavily on local inhibitory populations of neurons (Onslow *et al.*, 2014) and could

therefore be a more reliable indicator of an E-I imbalance in ASD than GBA. The observed reduction in PAC is therefore consistent with histological findings showing under-developed inhibitory interneurons (Casanova *et al.*, 2003) and an E-I imbalance in autism (Rubenstein and Merzenich, 2003). Affected local inhibitory processes could manifest as high-frequency 'noisy' activity and reduced signal-to-noise in perceptual systems, as reported in ASD (Casanova *et al.*, 2003; Rubenstein and Merzenich, 2003; Vilidaite *et al.*, 2017). However, it should be noted that further corroborating evidence will be required before a definitive link between PAC and E-I interactions can be established.

It has been proposed that dysregulated local activity could have concomitant effects on establishing patterns of inter-regional and global connectivity (Voytek and Knight, 2015). In the context of our current investigation of the autistic visual system, reduced local PAC in V1 could therefore reveal a dysfunctional relationship with V1-V4 inter-regional connectivity. Indeed, an exploratory analysis reported in Supplementary Fig. 4 revealed a correlation between negativity of DAI (predominance of alpha feedback connectivity) and the strength of PAC across groups. Whilst the control group in its majority showed increased feedback alpha and increased alpha-gamma PAC, the relationship for the ASD group was significantly more variable (Supplementary Fig. 4). However, because of the visual grating paradigm used and the limited samples tested here, future research is required to test the general claims that PAC acts as a general cortical mechanism for oscillatory multiplexing to link connectivity at the global and local scales (Canolty and Knight, 2010; Seymour *et al.*, 2017) and that this mechanism is specifically affected in autism (Kessler *et al.*, 2016).

Interestingly, we did not find a relationship between AQ or GSQ and PAC in the ASD group (Fig. 4C and D), although there was a relationship with alpha DAI (Supplementary Fig. 4). In addition to the discussed issues regarding sensitivity of the GSQ, PAC may be related to specific clinical features of autism rather than general autistic traits (see 'Limitations' section). Accordingly, a recent study reported a correlation between the social component of the Autism Diagnostic Observation Schedule (ADOS) and local PAC in an adolescent autistic sample (Mamashli *et al.*, 2018).

Neurocognitive models of perception

Our results link with emerging theories of typical perception. Predictive-coding accounts of cortical activity describe the passage of top-down predictions from higher to lower areas via feedback pathways, with prediction errors computed at each level of the hierarchy being passed forward via feedforward pathways (Friston, 2005). Predictive-coding accounts of autism suggest that differences in perception emerge from fewer or hyper-precise top-down predictions, such that perception is less influenced by prior knowledge and contextual cues (Pellicano and Burr, 2012; Palmer *et al.*, 2017). Despite limitations, our data support this proposal by showing reduced feedback connectivity in the visual cortex in autism. We propose that where top-down information flow is reduced, the perceptual system could be forced from predictive to reactive, with increased prediction error signalling and concomitant impacts on autistic symptoms (Kessler *et al.*, 2016). This is supported by the observed correlations between feedback connectivity (DAI) and AQ score (Fig. 4B) and between DAI and PAC (Supplementary Fig. 4) but requires further thorough investigation.

Clinical implications and limitations

We note three limitations to this study. First, we did not collect a formal clinical assessment of autism, e.g. the ADOS. We therefore implemented strict participant exclusion criteria, only including autistic participants with a confirmed clinical diagnosis of ASD or Asperger's syndrome. Between groups, there were significant differences in autistic and sensory traits (Table 1). However, upon closer inspection of GSQ data, the ASD group showed a mixture of hyper- and hypo-sensitive traits between different sensory modalities making precise brain-behavioural correlations problematic (Supplementary Fig. 6). This may explain the lack of relationship between oscillatory connectivity and GSQ scores in autism (Fig. 5A and C). Brain-behaviour relationships might be better assessed using psychophysical tests of visual perception (Ashwin *et al.*, 2009), combined with formal clinical assessments. Second, because of the relatively low number of participants tested in each group, it would be inappropriate to generalize our findings, at this time, to the entire ASD spectrum and beyond the current visual grating paradigm. In addition, a greater number of participants may be required to achieve the appropriate statistical power for brain-behaviour correlations. Nonetheless, our novel analysis approach has revealed interesting and predicted findings (Kessler *et al.*, 2016) despite quite a diverse high-functioning ASD sample (e.g. GSQ scores) and may therefore provide important findings, upon which future research can replicate and extend. Third, we constrained our connectivity analyses to two regions of interest (V1, V4) located early in the visual system, due to their hierarchical connectivity, and the low-level nature of the visual grating stimulus. However, we may have missed the opportunity to characterize more complex feedforward-feedback relationships in wider visual cortex. Future work should therefore include more regions of interest in combination with stimuli requiring participants to explicitly engage in feedback processing to constrain visual perception. This approach could be particularly useful with high-functioning individuals, and help characterize the neurophysiological basis of autistic perception (Kessler *et al.*, 2016; Robertson and Baron-Cohen, 2017).

Acknowledgements

We wish to thank the volunteers who gave their time to participate in this study, and Dr Jon Brock for intellectual contributions to experimental design.

Funding

The Wellcome Trust, Dr Hadwen Trust and Tommy's Fund for supporting research costs. R.A.S. was supported by a cotutelle PhD studentship from Aston University and Macquarie University. J.M.S. was supported by The Netherlands Organisation for Scientific Research (NWO Vidi: 864.14.011).

Competing interests

The authors have no competing interests to disclose. A version of this manuscript has been uploaded to the pre-print BioRxiv service.

Supplementary material

Supplementary material is available at *Brain* online.

References

Ashwin E, Ashwin C, Rhydderch D, Howells J, Baron-Cohen S. Eagle-eyed visual acuity: an experimental investigation of enhanced perception in autism. Biol Psychiatry 2009; 65: 17–21.

American Psychological Association. Diagnostic and statistical manual of mental disorders. Arlington: American Psychiatric Association; 2013.

Baron-Cohen S, Wheelwright S, Hill J, Raste Y, Plumb I. The "Reading the Mind in the Eyes" test revised version: a study with normal adults, and adults with Asperger syndrome or high-functioning autism. J Child Psychol Psychiatry 2001a; 42: 241–51.

Baron-Cohen S, Wheelwright S, Skinner R, Martin J, Clubley E. The autism-spectrum quotient (AQ): evidence from Asperger syndrome/high-functioning autism, males and females, scientists and mathematicians. J Autism Dev Disord 2001b; 31: 5–17.

Bastos AM, Litvak V, Moran R, Bosman CA, Fries P, Friston KJ. A DCM study of spectral asymmetries in feedforward and feedback connections between visual areas V1 and V4 in the monkey. Neuroimage 2015a; 108: 460–75.

Bastos AM, Vezoli J, Bosman CA, Schoffelen J-M, Oostenveld R, Dowdall JR, et al. Visual areas exert feedforward and feedback influences through distinct frequency channels. Neuron 2015b; 85: 390–401.

Bonaiuto JJ, Meyer SS, Little S, Rossiter H, Callaghan MF, Dick F, et al. Lamina-specific cortical dynamics in human visual and sensorimotor cortices. eLife 2018; 7: e33977.

Bonnefond M, Kastner S, Jensen O. Communication between brain areas based on nested oscillations. eneuro 2017; 4: e0153-16.2017.

Brock J, Brown CC, Boucher J, Rippon G. The temporal binding deficit hypothesis of autism. Dev Psychopathol 2002; 14: 209–24.

Brown C, Gruber T, Boucher J, Rippon G, Brock J. Gamma abnormalities during perception of illusory figures in autism. Cortex 2005; 41: 364–76.

Buzsáki G, Wang XJ. Mechanisms of gamma oscillations. Annu Rev Neurosci 2012; 35: 203–25.

Canolty RT, Knight RT. The functional role of cross-frequency coupling. Trends Cogn Sci 2010; 14: 506–15.

Casanova MF, Buxhoeveden D, Gomez J. Disruption in the inhibitory architecture of the cell minicolumn: implications for autisim. Neuroscientist 2003; 9: 496–507.

Chacko RV, Kim B, Jung SW, Daitch AL, Roland JL, Metcalf NV, et al. Distinct phase-amplitude couplings distinguish cognitive processes in human attention. NeuroImage 2018; 175: 111–21.

Cohen MX. Assessing transient cross-frequency coupling in EEG data. J Neurosci Methods 2008; 168: 494–9.

Colclough GL, Brookes MJ, Smith SM, Woolrich MW. A symmetric multivariate leakage correction for MEG connectomes. NeuroImage 2015; 117: 439–48.

Cornew L, Roberts TP, Blaskey L, Edgar JC. Resting-state oscillatory activity in autism spectrum disorders. J Autism Dev Disord 2012; 42: 1884–94.

Courchesne E, Pierce K. Why the frontal cortex in autism might be talking only to itself: local over-connectivity but long-distance disconnection. Curr Opin Neurobiol 2005; 15: 225–30.

Dhamala M, Rangarajan G, Ding M. Analyzing information flow in brain networks with nonparametric Granger causality. Neuroimage 2008; 41: 354–62.

Dinstein I, Heeger DJ, Lorenzi L, Minshew NJ, Malach R, Behrmann M. Unreliable evoked responses in autism. Neuron 2012; 75: 981–91.

Doesburg SM, Vidal J, Taylor MJ. Reduced theta connectivity during set-shifting in children with autism. Front Hum Neurosci 2013; 7: 785.

Essen VCD, Glasser MF, Dierker DL, Harwell J, Coalson T. Parcellations and hemispheric asymmetries of human cerebral cortex analyzed on surface-based atlases. Cereb Cortex 2012; 22: 2241–62.

Fischl B. FreeSurfer. Neuroimage 2012; 62: 774–81.

Friston K. A theory of cortical responses. Philos Trans R Soc Lond B Biol Sci 2005; 360: 815–36.

Glasser MF, Coalson TS, Robinson EC, Hacker CD, Harwell J, Yacoub E, et al. A multi-modal parcellation of human cerebral cortex. Nature 2016; 536: 171–8.

Granger CW. Investigating causal relations by econometric models and cross-spectral methods. Econometrica 1969; 37: 424–38.

Grice SJ, Spratling MW, Karmiloff-Smith A, Halit H, Csibra G, De Haan M, et al. Disordered visual processing and oscillatory brain activity in autism and Williams syndrome. Neuroreport 2001; 12: 2697–700.

Happé F. The weak central coherence account of autism. Handbook of autism and pervasive developmental disorders. 3rd edn., Vol. 1. New Jersey: John Wiley & Sons; 2005. p. 640–9.

Hillebrand A, Barnes GR. Beamformer analysis of MEG data. Int Rev Neurobiol 2005; 68: 149–71.

Hoogenboom N, Schoffelen J-M, Oostenveld R, Parkes LM, Fries P. Localizing human visual gamma-band activity in frequency, time and space. Neuroimage 2006; 29: 764–73.

Hughes JR. Autism: the first firm finding = underconnectivity? Epilepsy Behav. 2007; 11: 20–4.

Jenkinson M, Smith S. A global optimisation method for robust affine registration of brain images. Med Image Anal 2001; 5: 143–56.

Jobs EN, Falck-Ytter T, Bölte S. Local and global visual processing in 3-year-olds with and without autism. J Autism Dev Disord 2018; 48: 1–9.

Keown CL, Shih P, Nair A, Peterson N, Mulvey ME, Müller R-A. Local functional overconnectivity in posterior brain regions is associated with symptom severity in autism spectrum disorders. Cell Rep 2013; 5: 567–72.

Kessler K, Seymour RA, Rippon G. Brain oscillations and connectivity in autism spectrum disorders (ASD): new approaches to

methodology, measurement and modelling. Neurosci Biobehav Rev 2016; 71: 601–20.
Khan S, Gramfort A, Shetty NR, Kitzbichler MG, Ganesan S, Moran JM, et al. Local and long-range functional connectivity is reduced in concert in autism spectrum disorders. Proc Natl Acad Sci 2013; 110: 3107–12.
Khan S, Michmizos K, Tommerdahl M, Ganesan S, Kitzbichler MG, Zetino M, et al. Somatosensory cortex functional connectivity abnormalities in autism show opposite trends, depending on direction and spatial scale. Brain 2015; 138: 1394–409.
Kitzbichler MG, Khan S, Ganesan S, Vangel MG, Herbert MR, Hämäläinen MS, et al. Altered development and multifaceted band-specific abnormalities of resting state networks in autism. Biol Psychiatry 2015; 77: 794–804.
Klimesch W. Alpha-band oscillations, attention, and controlled access to stored information. Trends Cogn Sci 2012; 16: 606–17.
Leekam SR, Nieto C, Libby SJ, Wing L, Gould J. Describing the sensory abnormalities of children and adults with autism. J Autism Dev Disord 2007; 37: 894–910.
Mamashli F, Khan S, Bharadwaj H, Losh A, Pawlyszyn SM, Hämäläinen MS, et al. Maturational trajectories of local and long-range functional connectivity in autism during face processing. Hum Brain Mapp 2018; 39: 4094–104.
Maris E, Oostenveld R. Nonparametric statistical testing of EEG- and MEG-data. J Neurosci Methods 2007; 164: 177–90.
Mejias JF, Murray JD, Kennedy H, Wang X-J. Feedforward and feedback frequency-dependent interactions in a large-scale laminar network of the primate cortex. Sci Adv 2016; 2: e1601335.
Michalareas G, Vezoli J, Van Pelt S, Schoffelen J-M, Kennedy H, Fries P. Alpha-beta and gamma rhythms subserve feedback and feedforward influences among human visual cortical areas. Neuron 2016; 89: 384–97.
Mottron L, Dawson M, Soulieres I, Hubert B, Burack J. Enhanced perceptual functioning in autism: an update, and eight principles of autistic perception. J Autism Dev Disord 2006; 36: 27–43.
Oakley BF, Brewer R, Bird G, Catmur C. Theory of mind is not theory of emotion: A cautionary note on the Reading the mind in the eyes test. J Abnorm Psychol 2016; 125: 818.
Onslow ACE, Jones MW, Bogacz R. A canonical circuit for generating phase-amplitude coupling. PloS One 2014; 9: e102591.
Oostenveld R, Fries P, Maris E, Schoffelen J-M. FieldTrip: open source software for advanced analysis of MEG, EEG, and invasive electrophysiological data. Comput Intell Neurosci 2010; 2011: 156869. doi: 10.1155/2011/156869.
Orekhova EV, Stroganova TA, Nygren G, Tsetlin MM, Posikera IN, Gillberg C, Elam M. Excess of high frequency electroencephalogram oscillations in boys with autism. Biol Psychiatry 2007; 62: 1022–9.
Özkurt TE, Schnitzler A. A critical note on the definition of phase–amplitude cross-frequency coupling. J Neurosci Methods 2011; 201: 438–43.
Palmer CJ, Lawson RP, Hohwy J. Bayesian approaches to autism: towards volatility, action, and behavior. Psychol Bull 2017; 143: 521.
Peiker I, David N, Schneider TR, Nolte G, Schöttle D, Engel AK. Perceptual integration deficits in autism spectrum disorders are associated with reduced interhemispheric gamma-band coherence. J Neurosci 2015a; 35: 16352–61.
Peiker I, Schneider TR, Milne E, Schöttle D, Vogeley K, Münchau A, et al. Stronger neural modulation by visual motion intensity in autism spectrum disorders. PLoS One. 2015b; 10: e0132531.
Pellicano E, Burr D. When the world becomes 'too real': a Bayesian explanation of autistic perception. Trends Cogn Sci 2012; 16: 504–10.
Port RG, Anwar AR, Ku M, Carlson GC, Siegel SJ, Roberts TP. Prospective MEG Biomarkers in ASD: pre-clinical evidence and clinical promise of electrophysiological signatures. Yale J Biol Med 2015; 88: 25.
Raven JC, Court JH. Raven's progressive matrices and vocabulary scales. Oxford: Oxford Psychologists Press; 1998.
Richter CG, Thompson WH, Bosman CA, Fries P. Top-down beta enhances bottom-up gamma. J Neurosci 2017; 37: 6698–711.
Rippon G, Brock J, Brown C, Boucher J. Disordered connectivity in the autistic brain: challenges for the 'new psychophysiology'. Int J Psychophysiol 2007; 63: 164–72.
Roberts TP, Khan SY, Rey M, Monroe JF, Cannon K, Blaskey L, et al. MEG detection of delayed auditory evoked responses in autism spectrum disorders: towards an imaging biomarker for autism. Autism Res 2010; 3: 8–18.
Robertson CE, Baron-Cohen S. Sensory perception in autism. Nat Rev Neurosci 2017; 18: 671.
Robertson AE, Simmons DR. The relationship between sensory sensitivity and autistic traits in the general population. J Autism Dev Disord 2013; 43: 775–84.
Rubenstein JLR, Merzenich MM. Model of autism: increased ratio of excitation/inhibition in key neural systems. Genes Brain Behav. 2003; 2: 255–67.
Schoffelen J-M, Hultén A, Lam N, Marquand AF, Uddén J, Hagoort P. Frequency-specific directed interactions in the human brain network for language. Proc Natl Acad Sci 2017; 114: 8083–8.
Seymour RA, Rippon G, Kessler K. The detection of phase amplitude coupling during sensory processing. Front Neurosci 2017; 11: 487.
Simon DM, Wallace MT. Dysfunction of sensory oscillations in autism spectrum disorder. Neurosci Biobehav Rev 2016; 68: 848–61.
Spyropoulos G, Bosman CA, Fries P. A theta rhythm in macaque visual cortex and its attentional modulation. Proc Natl Acad Sci 2018; 115: E5614–23.
Sun L, Grützner C, Bölte S, Wibral M, Tozman T, Schlitt S, et al. Impaired gamma-band activity during perceptual organization in adults with autism spectrum disorders: evidence for dysfunctional network activity in frontal-posterior cortices. J Neurosci 2012; 32: 9563–73.
Takesaki N, Kikuchi M, Yoshimura Y, Hiraishi H, Hasegawa C, Kaneda R, et al. The contribution of increased gamma band connectivity to visual non-verbal reasoning in Autistic children: a MEG study. PloS one 2016; 11: e0163133.
Taulu S, Simola J. Spatiotemporal signal space separation method for rejecting nearby interference in MEG measurements. Phys Med Biol 2006; 51: 1759.
Van Essen DC, Ugurbil K, Auerbach E, Barch D, Behrens TEJ, Bucholz R, et al. The Human Connectome Project: a data acquisition perspective. Neuroimage 2012; 62: 2222–31.
Van Veen BD, van Drongelen W, Yuchtman M, Suzuki A. Localization of brain electrical activity via linearly constrained minimum variance spatial filtering. IEEE Trans Biomed Eng 1997; 44: 867–80.
Vilidaite G, Yu M, Baker DH. Internal noise estimates correlate with autistic traits. Autism Res 2017; 10: 1384–91.
Voytek B, Knight RT. Dynamic network communication as a unifying neural basis for cognition, development, aging, and disease. Biol Psychiatry 2015; 77: 1089–97.